Journal of Crystal Growth 323 (2011) 372–375

Contents lists available at ScienceDirect

Journal of Crystal Growth

journal homepage: www.elsevier.com/locate/jcrysgro

Strong crystal anisotropy of magneto-transport property in Fe_3Si epitaxial film

H.Y. Hung [a], S.Y. Huang [a,c], P. Chang [b], W.C. Lin [a], Y.C. Liu [a], S.F. Lee [c,*], M. Hong [b], J. Kwo [a,d,**]

[a] Department of Physics, National Tsing Hua University, Hsinchu 30013, Taiwan
[b] Department of Materials Science and Engineering, National Tsing Hua University, Hsinchu 30013, Taiwan
[c] Institute of Physics, Academia Sinica, Nankang, Taipei 115, Taiwan
[d] Center for Condensed Matter Sciences, National Taiwan University, Taipei 10617, Taiwan

ARTICLE INFO

Available online 18 November 2010

Keywords:
A1. Anisotropic magnetoresistance
A2. Single crystal growth
A3. Molecular beam epitaxy
B2. Fe_3Si
B2. GaAs
B2. Spintronics

ABSTRACT

This work reports the magneto-anisotropy property of epitaxial Fe_3Si film grown on GaAs (0 0 1) substrate by molecular beam epitaxy (MBE). We present a strong dependence of anisotropic magnetoresistance (MR) on field in the Fe_3Si film plane. The electron transport behavior is highly dependent on the direction of the current either parallel or perpendicular to the magnetic easy axis. By altering the direction of current from magnetic hard axis to magnetic easy axis, the unconventional behavior switches to normal anisotropic magnetoresistance (AMR). In addition, the anisotropic behaviors were also observed from the magneto-optic Kerr effect (MOKE) measurement, which demonstrates unusual anisotropic properties with the crystalline anisotropic constant $K_1=(3.8\pm0.2)\times10^4$ erg/cm^3 and uni-axial anisotropy $K_u=(1.2\pm0.04)\times10^4$ erg/cm^3. The ratio K_1/K_u was used to account for the MR.

1. Introduction

One of the key issues for the realization of spintronic applications is the attainment of high-quality epitaxial ferromagnets with high spin polarization on semiconductor substrates. The structural, transport, and magnetic properties of the Fe_3Si/GaAs heterostructures have been studied [1–7]. Fe_3Si is a ferromagnetic material that could be a promising candidate for injections of spin-polarized electrons from a ferromagnet into a semiconductor [8]. For Fe_3Si epitaxial films grown on GaAs (001) by MBE, the magneto-transport properties have been studied mostly by applying current along the magnetic hard axis, i.e., the [1 1 0] crystallographic axis, which is the easy cleavage direction for the (1 0 0) GaAs substrate [4,6]. Anisotropic magnetoresistance (AMR) of Fe_3Si showed the following unconventional behavior—the resistivity in a field perpendicular to the current was larger than that for resistivity in a field parallel to the current. In single crystals, the direction of both the current and the magnetization with respect to the crystal axes are known to affect the behavior of MR. [9]

In our present work, magneto-transport studies of epitaxial Fe_3Si films showed a strong anisotropic dependence of magnetoresistance (MR) in the film plane, and the behavior was highly dependent on the direction of the current with respect to the crystallographic axes. In addition, similar anisotropic behaviors were also observed from the MOKE measurement, which led to deductions of the crystal anisotropic constant K_1 and the uni-axial anisotropic constant K_u.

2. Experiment

High quality epitaxial Fe_3Si thin films were grown on the GaAs (0 0 1) surface in a multi-chamber MBE system that included a GaAs-based solid source growth chamber, an arsenic-free metal growth chamber, and ultrahigh vacuum (UHV) transfer modules interconnecting the MBE chambers. [1] The GaAs epi-layers were grown on GaAs (0 0 1) substrates at a temperature of 600 °C. The samples were then transferred in situ to the metal chamber to deposit Fe_3Si. Prior to the metal deposition, a Ga-stabilized surface with a 4×6 reconstructed pattern, monitored by reflection high-energy electron diffraction (RHEED) was obtained by heating the samples to 550 °C in an As-free metal chamber. Fe and Si were codeposited from high temperature effusion cells at a growth temperature of 250 °C with a base pressure of 1×10^{-9} Torr. The lattice constants of Fe_3Si nearly matched with those of GaAs, based on the high-resolution X-ray diffraction analysis. [3]. The transport properties of the resistivity and the magnetoresistance were measured by a standard four-probe technique in the cryostat with a superconducting magnet up to 9 T. Moreover, the longitudinal MOKE measurements were conducted ex-situ to characterize the in-plane magnetic anisotropy. The samples were mounted on a rotatable plate and freely rotated over 0°–360° with an error bar of 1° during the measurement.

* Corresponding author. Tel.: +886 2 2789 6767; fax: +886 2 2783 4187.
** Corresponding author. Tel.: +886 3 574 2800; fax: +886 3 572 3052.
E-mail addresses: leesf@phys.sinica.edu.tw (S.F. Lee), raynien@ntu.edu.tw (J. Kwo).

0022-0248/$ - see front matter © 2010 Elsevier B.V. All rights reserved.
doi:10.1016/j.jcrysgro.2010.11.075

3. Results and discussion

The AMR, which is related to the direction of the current and the orientation of the magnetization, is due to spin–orbit coupling. The AMR of ferromagnetic materials can be expressed as:

$$\rho = \rho_{\perp} + (\rho_{\parallel} - \rho_{\perp})\cos^2\theta_M \quad (1)$$

where θ_M denotes the angle between the direction of the current and magnetization; $\rho_{\perp}$ and $\rho_{\parallel}$ are the resistivity for the current is parallel and perpendicular to the magnetization, respectively. However, the magneto-transport properties reported so far for the Fe_3Si epitaxial films have been studied primarily by applying current along the magnetic hard axis, i.e., the [1 1 0] crystallographic axis, which is the easy cleavage direction for the (1 0 0) GaAs substrate [4,6]. An unusual behavior was observed where the resistivity for a field perpendicular to the current was larger than the resistivity that for a field parallel to the current. This may be understood on the fact that the magnetization lies in the easy axis at a low field and lags in the external field direction. [4] Our measurement for the angular dependence of resistivity with a current along the [1 1 0] axis for a sample of 21 nm thick is shown in Fig. 1 under 500 Oe at $T=100$ K. θ_H in Fig. 1 is the angle between the current direction and the magnetic field. The error bar of resistivity due to electrical measurements is less than 0.01%, but the error bar from geometry estimation could be as large as 10%. The resistivity showed a zigzag behavior as previously reported [4,6], which showed maximum and minimum values for the magnetic field perpendicular and parallel to the current direction, respectively. This behavior indicated a single-domain magnetization rotation under the influence of a strong magnetic field and crystalline anisotropy.

The magnetic field sweeps of MR at 100 K at different fixed angles of θ_H are shown in Fig. 2(a), where the value at 2 T is about 0–0.5%, which is similar to recent reports. [6] The MR ratio is defined by [10]

$$MR(\%) = [\rho(H) - \rho(0)]/\rho(0) \times 100 \quad (2)$$

where $\rho(0)$ and $\rho(H)$ are the resistivity at zero field and at field H, respectively. The negative MR and the linear slope were observed at all angles in a high magnetic field. For magnetic alloys, the negative MR may be attributed to the effective field acting on the localized spins that suppressed the fluctuation of spins by increasing the magnetic field. [6] The low-field MR between -500 and 500 Oe showed a hysteretic behavior with the resistance peaks occurring at the coercive field H_c, which corresponds to the maximum disorder of the distribution of magnetic domains, as shown in Fig. 2(b). As the field became smaller, the magnetic field was not strong enough to align the magnetic moment in the direction of field. Hence, the magnetic moment deviated from the orientation of the magnetic field to the easy axis, which then led all of the MR curves at different angles to converge toward the same magnetic resistivity at a low field around a θ_H of 62°. The angle was not 45°, and therefore suggested evidence of a hard uni-axial axis in addition to a four-fold hard axis, as further supported by the following MOKE measurement.

The hysteresis loops measured by MOKE showed a strong uni-axial anisotropy. The polar plots of the magnetizing energy ω calculated from the integration of hysteresis loops are shown as dashed lines in Fig. 3. Clearly, there is a four-fold symmetry coexisting with a strong uni-axial symmetry. The experimental data was fitted with the formula [11]

$$\omega(\theta) = K_0 + \frac{K_1}{4}\sin^2\left(2\left(\theta - \frac{\pi}{4}\right)\right) + K_u\sin^2\left(\theta - \frac{\pi}{2}\right) \quad (3)$$

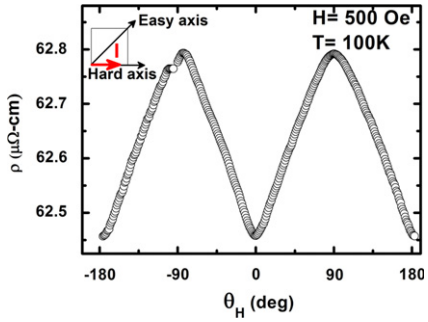

Fig. 1. Angular dependence of resistivity at 100 K for an applied field $H=500$ Oe. The current direction is parallel to the hard axis [1 1 0] (see inset).

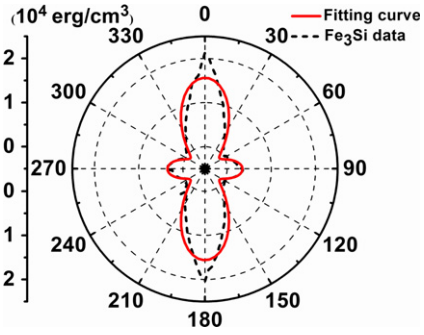

Fig. 3. Anisotropic energy at different angles relative to the strong uni-axial hard axis. The dashed line is calculated from the integration of MOKE hysteresis loops and the solid line is the fitting curve to the data.

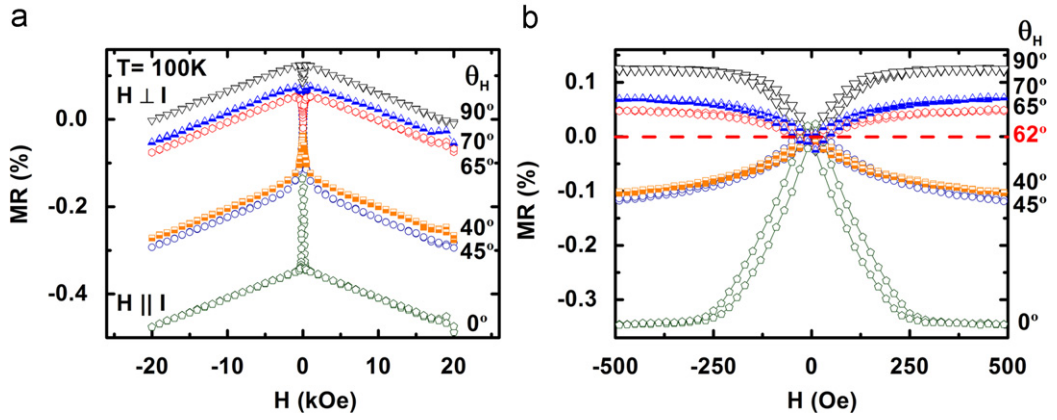

Fig. 2. (a) High field and (b) low field MR vs. applied field H for several angles (θ, in degrees) at $T=100$ K. The current direction is parallel to the hard axis [1 1 0].

where K_0, K_1, K_u, and θ represent the constant independent of the angle, the crystal anisotropy constant, the uni-axial anisotropy constant, and the angle between the magnetization and coordinate axis, respectively. The solid line shows the fitting result of the experimental data, where $K_1=(3.8\pm0.2)\times10^4$ erg/cm^3 and $K_u=(1.2\pm0.04)\times10^4$ erg/cm^3. The value of K_1 is close to the bulk value $K_{1(\mathrm{bulk})}=5.4\times10^4$ erg/cm^3 [12] and is similar to the value reported for Fe_3Si. [13,14] The K_u is the same order of magnitude as K_1, which resulted in a strong uni-axial contribution from the Fe_3Si films and led to the two non-equivalent magnetic hard axes [15]. The uni-axial anisotropy was also related to the Fe concentration and the thickness of the Fe_3Si film [13,14]. However, to clarify the reason for the results of the strong uni-axial anisotropic property, samples with different Fe concentrations and thicknesses must be studied. The angle between the strong uni-axial axis and the easy axis can be determined by [16]

$$\cos 2\theta = -|K_u/K_1| \quad \text{for} \quad |K_u/K_1| \le 1$$

We found that the angle was about $(54.4^\circ\pm0.7^\circ)$, which is close to an angle of 62° from the transport measurement of the angular dependence of *MR* with current along the magnetic hard axis. The small deviation may be attributed to the misalignment when placing the electrical contacts.

By changing the current direction along the hard axis to the easy axis, we found that the angular dependence of the resistivity displayed a step-like behavior for the magnetic field below 100 Oe. Resistivity jump occurred when the moment, which originally lay along one easy axis, rotated to lie along the other easy axis. At high fields above 500 Oe, the resistivity curve reached maximum and minimum values for the magnetic field parallel and perpendicular to the current, respectively. This can be described by $\cos^2\theta$ as the conventional AMR effect (see Fig. 4(a) and (b)). The *MR* curves measured as a function of the field at different angles also showed a negative *MR* and linear slope in the high magnetic field as shown in Fig. 5(a). The *MR* curves demonstrated a two-jump behavior at the values of 0° and 90° in the range of ±50 Oe as shown in Fig. 5(b), indicating the four-fold symmetry of the Fe_3Si crystal. In the beginning, the magnetic field was strong enough to align magnetic moments and led to a larger and small MR at the values of 0° and 90°, respectively. As the field was reduced gradually, the moment jumped from one easy axis to the other easy axis. This two-jump behavior was also obtained for the *MR* at different angles. A wide plateau was observed at intermediate angles, indicating that the magnetic moment stayed along one easy axis over a fairly large range of magnetic field until the field was large enough to overcome the energy barrier of the hard axis. These results demonstrated the unusual anisotropic behavior in our Fe_3Si films.

4. Conclusion

Our study on epitaxial Fe_3Si films showed the unusual zigzag behavior of the angular dependence of resistivity when the current was applied along the magnetic hard axis. By altering the current

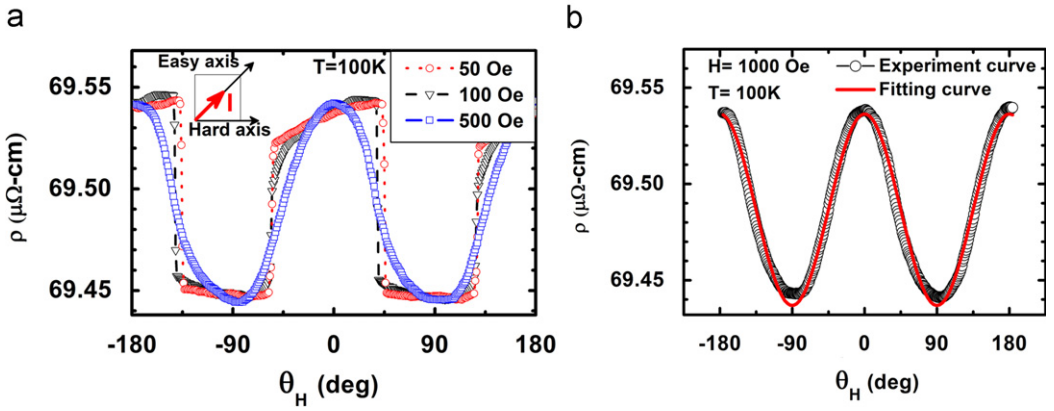

Fig. 4. Angular dependence of resistivity at 100 K for (a) several low fields and (b) $H=1000$ Oe. The direction of current is parallel to the easy axis [1 0 0] (see inset). The solid line in (b) is the best fit with the function $\cos^2(\theta_M)$.

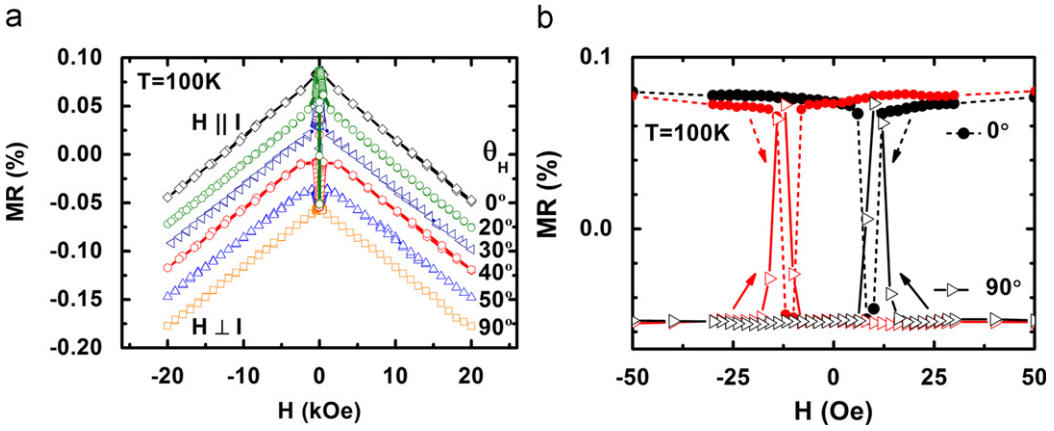

Fig. 5. (a) High field *MR* at several angles and (b) low field *MR* at 0° and 90° (θ, in degrees) vs. applied field H at $T=100$ K. In (b), the solid circle and dashed line are for 0° and the hollow triangle and solid line are for 90°. The current direction is parallel to the easy axis [1 0 0].

direction from the magnetic hard axis to the magnetic easy axis, the resistivity showed the $\cos^2(\theta_M)$ behavior of the conventional AMR effect. Moreover, the MR showed a step function behavior at a low field, indicating the four-fold symmetry of the Fe_3Si crystallographic axes. Large anisotropic constants of K_1 and K_u were deduced from the MOKE measurement, which led to the asymmetric AMR behavior. Based on the K_1/K_u ratio, the angle between the four-fold easy axis and strong uni-axial hard axis was determined, consistent with the magnetic transport measurement. Our current findings would be useful for further magnetic switching applications, and open new approaches for the realization of spin injection from Fe_3Si into GaAs.

Acknowledgment

The authors wish to thank the National Science Council of Taiwan for supporting this work under the grant of NSC-96- 2628-M-007-003-MY3.

References

[1] M. Hong, H.S. Chen, J. Kwo, A.R. Kortan, J.P. Mannaerts, B.E. Weir, L.C. Feldman, J. Cryst. Growth 111 (1991) 984.
[2] S.H. Liou, S.S. Malhotra, J.X. Shen, M. Hong, J. Kwo, H.S. Chen, J.P. Mannaerts, J. Appl. Phys. 73 (1993) 6766.
[3] Y.L. Hsu, Y.J. Lee, Y.H. Chang, M.L. Huang, Y.N. Chiu, C.C. Ho, P. Chang, C.H. Hsu, M. Hong, J. Kwo, J. Cryst. Growth 301–302 (2007) 588.
[4] M. Bowen, K.-J. Friedland, J. Herfort, H.-P. Schönherr, K.H. Ploog, Phys. Rev. B 71 (2005) 172401.
[5] J. Thomas, J. Schumann, H. Vinzelberg, E. Arushaov, R. Engelhard, O.G. Schmidt, T. Gemming, Nanotechnology 20 (2009) 235604.
[6] H. Vinzelberg, J. Schumann, D. Elefant, J. Thomas, E. Arushanov, O.G. Schmidt, J. Appl. Phys. 104 (2008) 093707.
[7] A. Ionescu, C.A.F. Vaz, T. Trypiniotis, C.M. Gurtler, H. Garcia-Miquel, J.A.C. Bland, M.E. Vickers, R.M. Dalgliesh, S. Langridge, Y. Bugoslavsky, Y. Miyoshi, L.F. Cohen, K.R.A. Ziebeck, Phys. Rev. B 71 (2005) 094401.
[8] A. Kawaharazuka, M. Ramsteiner, J. Herfort, H.-P. Schönherr, H. Kostial, K.H. Ploog, Appl. Phys. Lett. 85 (2004) 3492.
[9] R.P. vanGorkom, J. Caro, T.M. Klapwijk, S. Radelaar, Phys. Rev. B 63 (2001) 134432.
[10] C. Robert, O'Handley, Modern Magnetic Material: Principles and Applications, Wiley Interscience, New York, 2000, p. 579.
[11] D. Spoddig, U. Köhler, M. Haak, M. Kneppe, T. Schmitte, A. Westphalen, K. Theis-Bröhl, R. Meckenstock, D. You, J. Pelzl, Superlattices Microstruct. 43 (2008) 180.
[12] M. Goto, T. Kamimori, J. Phys. Soc. Jpn. 52 (1983) 3710.
[13] K. Lenz, E. Kosubek, K. Baberschke, H. Wende, J. Herfort, H.-P. Schönherr, K.H. Ploog, Phys. Rev. B 72 (2005) 144411.
[14] J. Herfort, H.-P. Schönherr, B. Jenichen, J. Appl. Phys. 103 (2008) 07B506.
[15] M. Brockmann, M. Zölfl, S. Miethaner, G. Bayreuther, J. Magn. Magn. Mater. 198–199 (1999) 384.
[16] C. Daboo, R.J. Hicken, D.E.P. Eley, M. Gester, S.J. Gray, A.J.R. Ives, J.A.C. Bland, J. Appl. Phys. 75 (1994) 5586.